

## **Supplementary Information: Onchocerciasis-associated skin and ocular disease and the impact of ivermectin treatment on morbidity prevalence: a modelling study**

Matthew A. Dixon<sup>1†\*</sup>, Aditya Ramani<sup>1,2†</sup>, Martin Walker<sup>1,2</sup>, Jacob N. Stapley<sup>1</sup>, Michele E. Murdoch<sup>3</sup>, Ian E. Murdoch<sup>4</sup>, Gladys A. Ozoh<sup>5</sup>, Jonathan F. Mosser<sup>6,7</sup>, Maria-Gloria Basáñez<sup>1\*</sup>

<sup>1</sup>MRC Centre for Global Infectious Disease Analysis and London Centre for Neglected Tropical Disease Research, Department of Infectious Disease Epidemiology, School of Public Health, Imperial College London, 90 Wood Lane, London, W12 0BZ, UK

<sup>2</sup>Department of Pathobiology and Population Sciences, Royal Veterinary College, Hawkshead Lane, Hatfield, Hertfordshire, AL9 7TA, UK

<sup>3</sup>Department of Dermatology, West Herts Teaching Hospitals NHS Trust, Watford, Herts., UK

<sup>4</sup>International Centre for Eye Health, Institute of Ophthalmology, London, UK

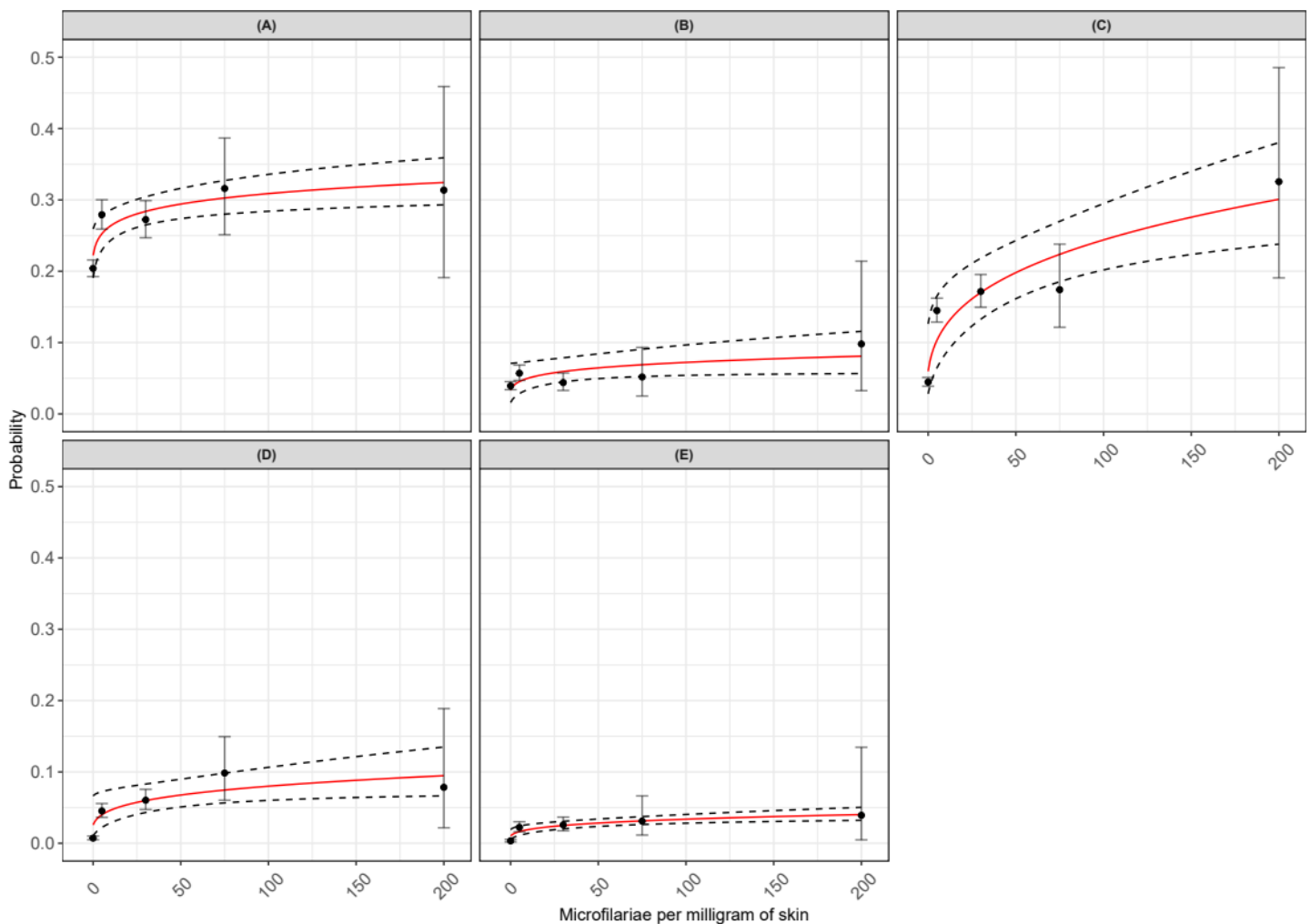
<sup>5</sup>Dermatology Division, University of Nigeria Teaching Hospital, Ituku Ozala Enugu State, Nigeria

<sup>6</sup>Institute for Health Metrics and Evaluation, Hans Rosling Center for Population Health, 3980 15th Ave NE, Seattle WA 98195, USA

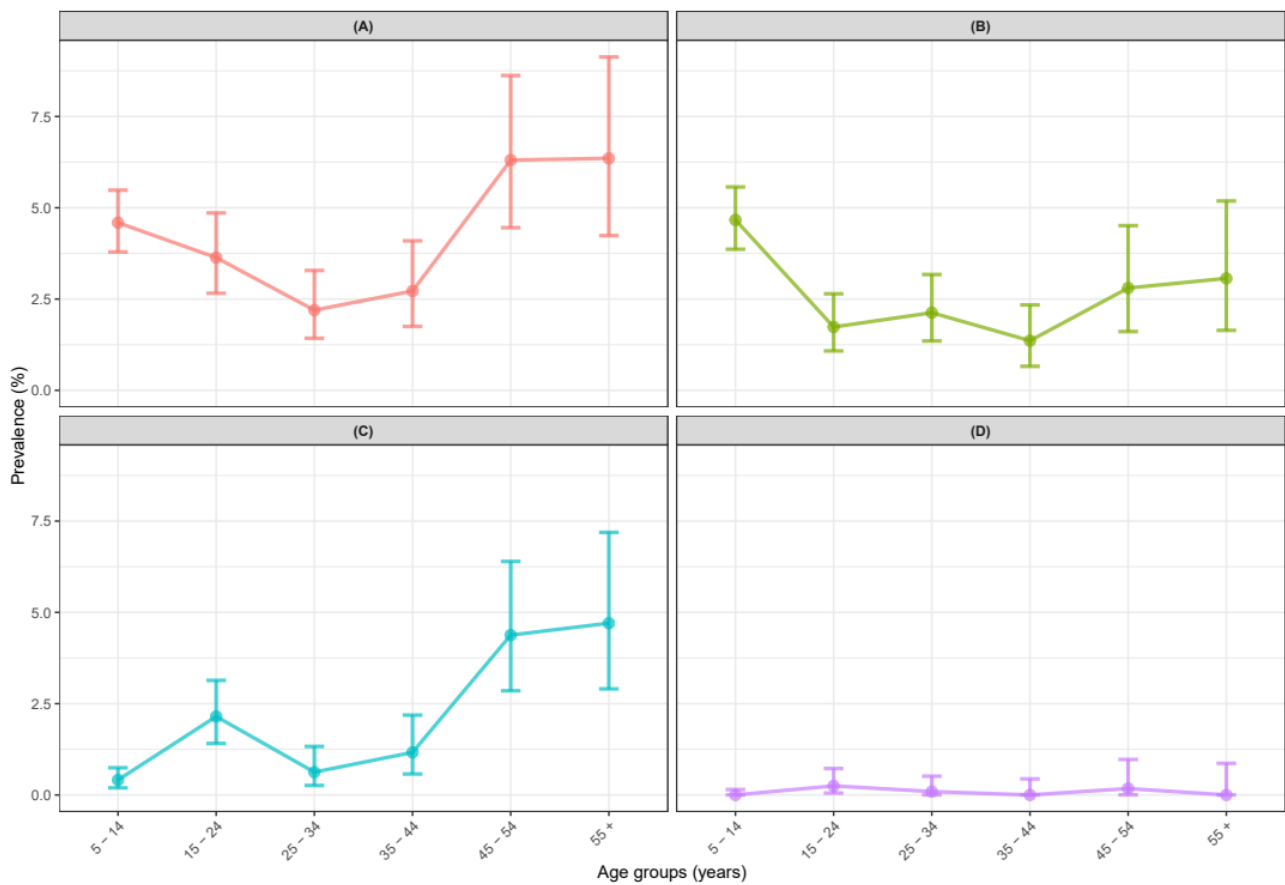
<sup>7</sup>Department of Global Health, School of Public Health, and Seattle Children's Hospital, University of Washington, Seattle WA, USA

†Contributed equally

\*Corresponding authors: [m.dixon15@imperial.ac.uk](mailto:m.dixon15@imperial.ac.uk) (MAD) and [m.basanez@imperial.ac.uk](mailto:m.basanez@imperial.ac.uk)



**Supplementary Fig. 1. Probabilities of developing onchocerciasis skin disease (OSD) sequelae as a function of microfilarial load.** Black circles are estimates from Murdoch et al.<sup>1</sup> with Clopper-Pearson 95% confidence intervals<sup>2</sup>; red lines represent a generalized linear model (GLM) with a log-link function fitted to the data using R v.4.3.2 (<https://cran.r-project.org/bin/windows/base/>); dashed lines are the 95% confidence intervals around model predictions. The GLM is  $Y(M_{(i)}) = \exp\{\beta_1[\log(M_{(i)} + 1)] + \beta_0\}$  where  $Y(M_{(i)})$  represents the probability of developing each OSD sequela as a function of  $M_{(i)}$ , the individual's microfilarial load (mean no. of mf/mg) from two iliac crest snips taken from each individual;  $M_{(i)}$  is taken as the mid-point of the binned mean microfilarial load according to the bins (0 to <1, 1 to <10, 10 to <50, 50 to <100,  $\geq 100$ ) presented in the Supplementary File S1 of Murdoch et al.<sup>1</sup>;  $\beta_0$  is the intercept, such that a microfilarial load of zero can be associated with a non-zero OSD probability (to account for sampling error in the skin-snipping process), and  $\beta_1$  is the strength of the association between microfilarial load and the probability of developing OSD. **A** Severe itch ( $\beta_0 = -1.504$ ;  $\beta_1 = 0.071$ ). **B** Reactive skin disease ( $\beta_0 = -3.390$ ;  $\beta_1 = 0.165$ ). **C** Atrophy ( $\beta_0 = -2.817$ ;  $\beta_1 = 0.305$ ). **D** Depigmentation ( $\beta_0 = -3.659$ ;  $\beta_1 = 0.246$ ). **E** Hanging groin ( $\beta_0 = -4.571$ ;  $\beta_1 = 0.256$ ).



**Supplementary Fig. 2. Age-prevalence profiles for the reversible onchocerciasis skin disease sequelae within the reactive skin disease category.** Circles are prevalence estimates from Murdoch et al.<sup>1</sup> with Clopper-Pearson 95% confidence intervals<sup>2</sup>. **A** RSD: Reactive skin disease. **B** APOD: Acute papular onchodermitis. **C** CPOD: Chronic papular onchodermitis. **D** LOD: Lichenified onchodermitis.

## Supplementary Text 1. Further EPIONCHO-IBM details

### Exposure heterogeneity and density dependence

The stochastic, individual-based EPIONCHO-IBM<sup>3</sup> has been developed from its deterministic, population-based (EPIONCHO) predecessors<sup>4-7</sup>. The model tracks, in a closed population (of 2,000 individuals for this work), the number of male and (fertile/non-fertile) female *Onchocerca volvulus* adult worms in human hosts (modelled using stochastic difference equations); the number of skin microfilariae (per mg of skin or per skin snip, modelled deterministically by using a partial differential equation that accounts for the contribution of each age class of adult female worms to the number of microfilariae in individuals assuming a worm's age-specific fecundity rate), and the number of infective, L3 larvae in blackfly vectors (modelled deterministically). EPIONCHO-IBM generates a 'true' microfilarial load and an 'observed' microfilarial load (taking into account skin-snip sensitivity)<sup>3</sup>. Parasite population abundance is regulated in humans and flies by density-dependent processes operating upon establishment of incoming worms within humans; establishment of L3 larvae within vectors, and vector survival<sup>5</sup>. Excess mortality of humans as a function of their microfilarial load<sup>8,9</sup> has not yet been included. For sub-Saharan Africa settings, the model has been parameterised for savannah *O. volvulus*–*S. damnosum* sensu lato (s.l.)<sup>3,5,6</sup>. The baseline (pre-control) microfilarial prevalence (indicative of the endemicity level) is determined by the annual biting rate (ABR, no. bites/person/year)<sup>3,6</sup>. Unless vector control is explicitly modelled, the transmission conditions are assumed to remain constant throughout the simulations in the absence of robust data to indicate changes in vector density or secular trends due to environmental change.

Individuals within the model are differentially exposed to blackfly bites depending on their age and sex<sup>4,10</sup> as well as on their individual specific exposure,  $E_{(i)}$ . This individual exposure factor is assigned at birth and drawn from a gamma distribution,

$$E_{(i)} \sim G(k_E, \beta_E) \quad \text{Eqn. (S1)}$$

where  $k_E$  is the shape parameter and  $\beta_E$  the rate parameter. It is assumed that  $k_E = \beta_E$ , such that the mean exposure in the population is unity, i.e., blackfly bites are distributed among hosts with an average exposure given by the ABR<sup>3</sup>. The  $k_E$  parameter defines the degree of inter-individual exposure heterogeneity, whereby lower values of  $k_E$  represent stronger overdispersion in exposure heterogeneity and vice-versa. In this work we used  $k_E$  values equal to 0.3 or 0.4<sup>3</sup>.

Parasite population regulation is assumed to depend on parasite density. Density-dependent processes are important in helminth transmission dynamics, as they contribute to parasite

population stability and resilience to interventions<sup>11,12</sup>. In EPIONCHO-IBM, density dependence is assumed to operate upon the establishment and development to the infective L3 stage of ingested microfilariae within blackflies, whose survival is also affected by the density of microfilarial intake (a function of the intensity of microfilaridermia in the human host)<sup>5</sup>. Parasite establishment within humans is assumed to depend on transmission intensity, measured by the annual transmission potential (ATP, the no. of L3 larvae potentially received per person per year, which in the model is a function of the ABR and the mean no. of L3 per blackfly)<sup>3,5,6,13</sup>. Different values of  $k_E$  are associated with different values of the parameters describing the establishment and development to adult worms of the L3 larvae transmitted from vectors to humans, as follows,

| Shape parameter of gamma distribution | Density dependence parameters for parasite establishment within humans |                     |       |
|---------------------------------------|--|---------------------|-------|
| $k_E$                                 | $\delta_{H_0}$   | $\delta_{H_\infty}$ | $c_H$ |
| 0.2                                   | 0.385  | 0.003               | 0.008 |
| 0.3                                   | 0.186  | 0.003               | 0.005 |
| 0.4                                   | 0.118  | 0.002               | 0.004 |

Where  $\delta_{H_0}$  is the proportion of L3 larvae developing to adult worms within the human host, per bite, when ATP tends to 0;  $\delta_{H_\infty}$  is the proportion of L3 larvae developing to adult worms within the human host, per bite, when ATP is very large, and  $c_H$  is the severity of transmission intensity-dependent parasite establishment within humans. A full description of EPIONCHO-IBM can be found in Hamley et al.<sup>3</sup>.

### Treatment coverage and proportion of never-treated population

We used the controlled treatment correlation approach proposed by Dyson et al.<sup>14</sup>, whereby each individual in the population is assigned a probability of attending any round, drawn from a Beta distribution. The correlation parameter ( $\rho$ ) controls the magnitude of correlation between attendance to consecutive treatment rounds by individuals and is related to the Beta distribution  $\alpha$  and  $\beta$  parameters following the expressions:

$$\alpha = c(1 - \rho)/\rho \text{ and } \beta = (1 - c)(1 - \rho)/\rho \quad \text{Eqns. (S2, S3)}$$

where  $c$  is the coverage of total population (Matthew Graham, pers. comm.). A  $\rho$  value of 0 indicates no correlation between the treatment rounds attended by an eligible individual (with eligibility assigned according to individuals' age; children under the age of 5 years do not receive treatment), such that individuals are randomly assigned to receiving treatment at each round. (NB when  $\rho = 0$  we cannot divide by zero, so the model assumes that treatment is random with coverage  $c$ .) A  $\rho$  value of 1 indicates a fully systematic scheme such that those

individuals which are assigned to receiving treatment in round 1 will always receive treatment in subsequent rounds. Specifying  $\rho$  values between 0 and 1 allows for a lesser or greater degree of systematic treatment adherence in the simulated treatment programme. In addition, a fixed proportion of the eligible population was randomly assigned to never receiving treatment, which was required to attain the never-treated proportion reported after 5 or 6 treatment rounds in the study sites of Taraba (Nigeria) and Bushenyi (Uganda)<sup>15</sup> (see Table 2 of Main Text and Supplementary Fig. 5).

## **Supplementary Text 2. Integration of onchocerciasis skin disease sequelae (OSD) into EPIONCHO-IBM**

At every daily time-step in the model, individuals are at risk of developing OSD sequelae if the criteria of being currently sequela-negative and microfilaria (mf)-positive are satisfied (Fig. 1 in Main Text). For the reversible and irreversible OSD sequelae, we assumed that individuals under the age of two years would not be able to develop such sequelae. Since the pre-patent period of *Onchocerca volvulus* is 2-3 years<sup>16</sup>, we assumed that individuals needed to be at least 2 years old before they could become OSD sequela-positive. Those individuals at risk of developing OSD sequelae undergo a Bernoulli trial with (daily) probabilities of developing each sequela given in Table 1 of the Main Text. For the reversible conditions, individuals revert to being sequela-negative after a duration of 3 days which, after testing periods between 1 and 5 days, was the most consistent with the age-prevalence OSD profiles presented in Fig. 3 (Main Text). Individuals remain sequela-positive for the irreversible conditions.

For both reversible and irreversible sequelae, we ignore any age-dependent variation in exposure and/or susceptibility to developing disease, such as increasing risk from past infection or changing susceptibility with age.

For reversible OSD, we assumed that sequelae would be sufficiently transient that prevalence (after subtracting background morbidity) reflects underlying incidence and that any accumulation of past morbidity is negligible.

For irreversible OSD, we assumed that infected (microfilaria-positive) individuals have experienced a daily risk of developing the sequelae for a period equal to the average age of the sampled population (which was 25 years in the dataset we used<sup>1</sup>), subtracting the first 2 years of life, when it is assumed that morbidity cannot develop (Eqn. (1) in Main Text).

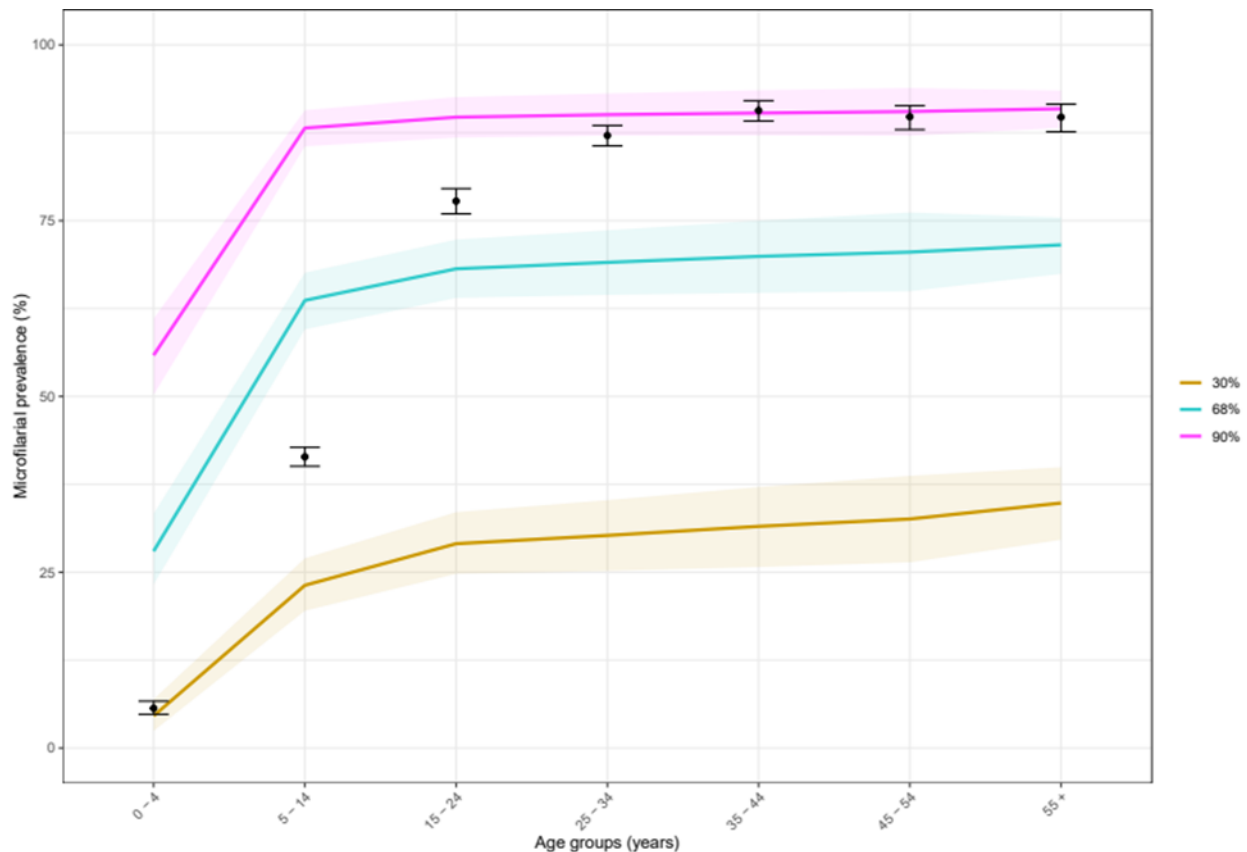
### **Supplementary Text 3. Integration of onchocerciasis ocular disease sequelae (OOD) into EPIONCHO-IBM**

At every daily time-step in the model, individuals are at risk of developing blindness if the criteria of being not currently blind or not assigned to become blind in the next two years, and having a non-zero ‘true’ microfilarial count are satisfied. We assume a delay of 2 years between being at risk of developing blindness and harbouring a given microfilarial load, such that microfilarial load 2 years in the past, and not current microfilarial load determines blindness risk<sup>17</sup>. In Eqn (2) of the Main Text, adapted from Little et al.<sup>17</sup>, the probability of blindness onset is related to an individual’s measurable (by skin snip) microfilarial count. However, in the model we identified individuals at risk of developing blindness based on their ‘true’ microfilarial count, rather than their count according to detectable microfilariae by skin-snip microscopy (see Supplementary Text 1, Exposure heterogeneity and density dependence), enabling the model to generate small blindness probabilities in those individuals with false negative microfilarial measurements. Those individuals at risk of developing blindness undergo a Bernoulli trial to determine whether they will become blind (2 years later).

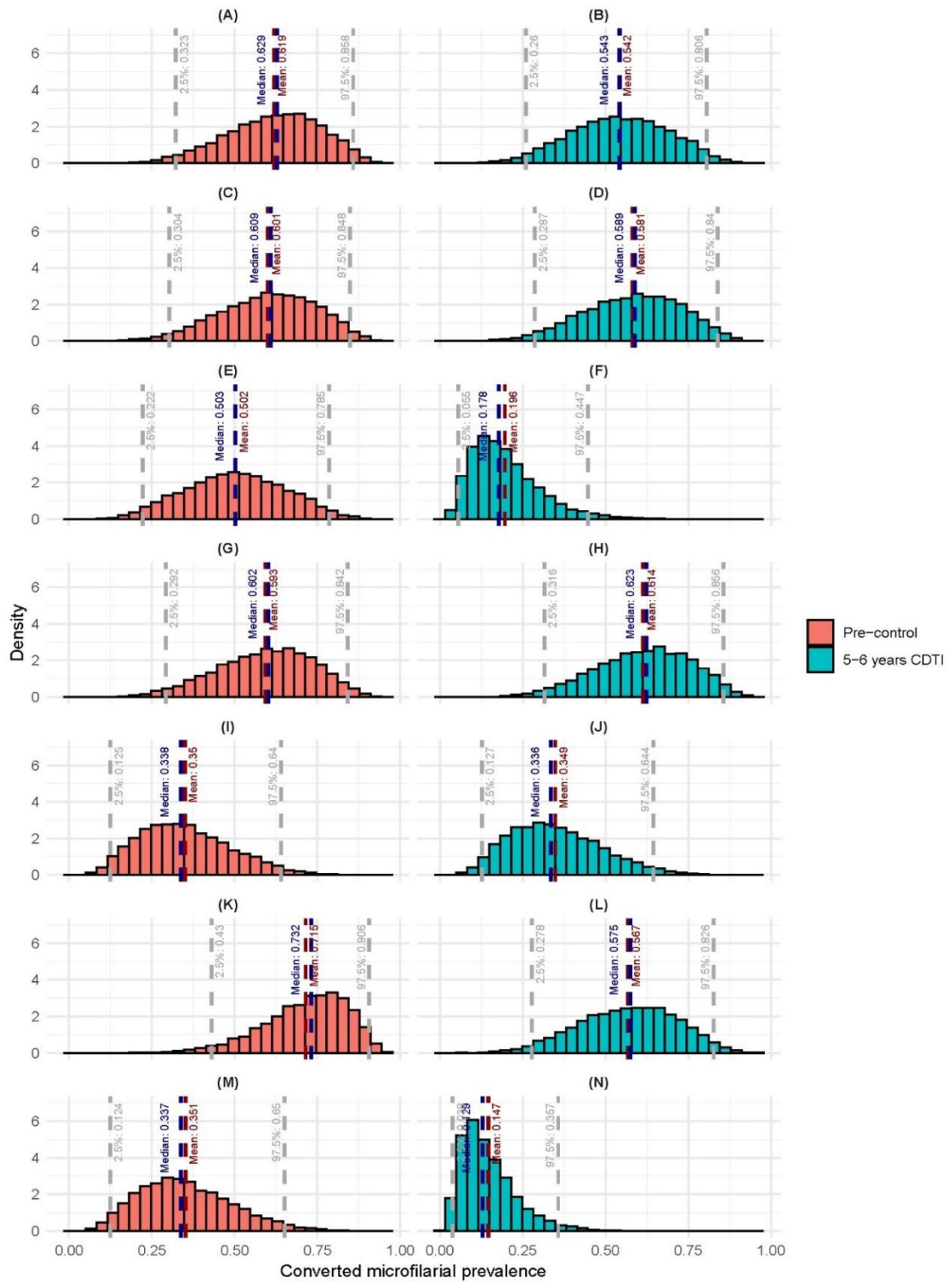
### **Supplementary Text 4. Converting nodule prevalence into microfilarial prevalence**

We used the procedure described by Coffeng (2024) in the Zenodo repository <https://zenodo.org/records/13969100><sup>18</sup>. This repository provides a set of posterior distribution draws (posterior\_sample.csv) and instructions for their use (posterior\_sample\_instructions.docx) to convert onchocercal nodule prevalence in adult males (aged  $\geq 20$  years) into microfilarial prevalence in the general population (aged  $\geq 5$  years). The posterior draws are based on the analysis of (paired) field data on prevalence of nodules and skin microfilariae from onchocerciasis-endemic villages presented in Coffeng et al. (2013)<sup>19</sup>, and in particular on the detailed description of the statistical model given in Supplementary S1 Text<sup>19</sup>. Briefly, the conditional distribution of village-level microfilarial prevalence given nodule prevalence is formulated using (univariate or multivariate) normal distributions for the logit-transformed prevalences (parameterised in terms of mean and variance or covariance). The observed, ‘apparent’ nodule prevalence is corrected according to the diagnostic performance parameters of nodule palpation to provide ‘true’ nodule prevalence. The comma-separated “posterior\_sample.csv” file<sup>18</sup> contains a large sample of draws from the joint posterior distribution of the vector of overall mean microfilarial prevalence and nodule prevalence and its covariance, village-level standard deviation of microfilarial and nodule prevalence and their

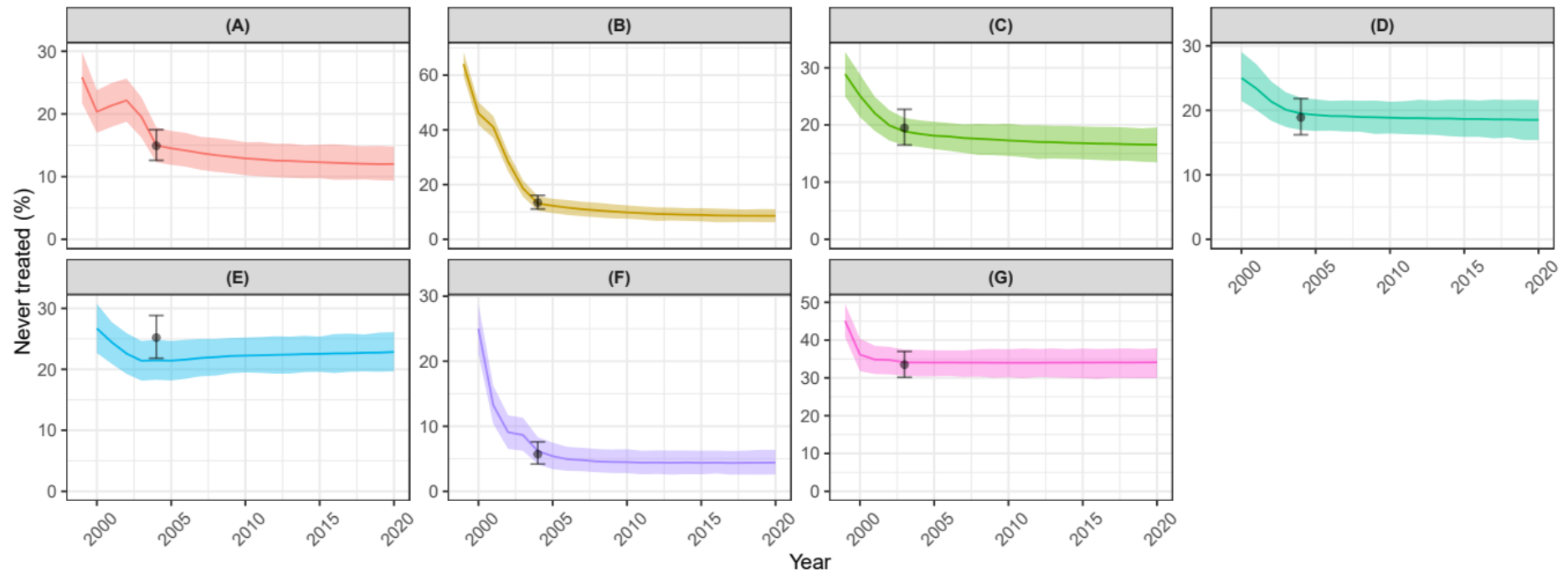
correlation, and specificity of nodule palpation. An algorithm is provided in the “posterior\_sample\_instructions.docx” file to generate a posterior predictive draw for microfilarial prevalence, conditional on a posterior draw of nodule prevalence<sup>18</sup>.



**Supplementary Fig. 3. Age-prevalence profiles of *Onchocerca volvulus* skin microfilariae in the Onchocerciasis Control Programme in West Africa.** Age-prevalence profiles were generated using EPIONCHO-IBM with annual biting rate (ABR) of 285, 2,000 and 60,000 bites/person/year and individual exposure parameter  $k_E = 0.3$  for, respectively, microfilarial prevalence of 30%, 68% and 90% for data from Kirkwood et al.<sup>20</sup>. Solid lines are the means of 1,000 model runs; shaded areas are the 95% uncertainty intervals (2.5th to 97.5th quantiles of stochastic model predictions); black circles are prevalence estimates with Clopper-Pearson 95% confidence intervals<sup>2</sup>.



**Supplementary Fig. 4. Posterior distributions of converted microfilarial prevalence from nodule prevalence.** Distributions were generated from nodule prevalence estimates collected before the implementation of community-directed treatment with ivermectin (CDTI) (pre-control) and 5–6 years into the CDTI programme in seven sites across Cameroon: **A, B** Kumba (rainforest). **C, D** Ngambe (forest-savannah mosaic). Nigeria: **E, F** Cross River (rainforest). **G, H** Kogi (forest-savannah mosaic). **I, J** Taraba (savannah). Sudan: **K, L** Raja (savannah). Uganda: **M, N** Bushenyi (rainforest). Data are from Ozoh et al.<sup>15</sup>. The conversion of nodule into microfilarial prevalence was conducted according to Coffeng<sup>18</sup> and Coffeng et al.<sup>19</sup> (see Supplementary Text 4). Light grey dashed lines indicate 95% credible intervals; dark blue dashed lines correspond to the medians, and dark red dashed lines indicate the means of the distributions. The median values of microfilarial prevalence were used to determine the annual biting rates (ABR, no. bites/person/year) necessary to simulate the baseline epidemiological conditions in the seven study sites (Table 2 of the Main Text).



**Supplementary Fig. 5. Modelled proportions (in percent) of never-treated population compared to data across seven study sites.** Cameroon: **A** Kumba. **B** Ngambe. Nigeria: **C** Cross River. **D** Kogi. **E** Taraba. Sudan: **F** Raja. Uganda: **G** Bushenyi. The trajectories of the modelled proportions of never-treated population are based on the estimations of the correlation parameter  $\rho$  as described in Supplementary Text S1 (Treatment coverage and proportion of never-treated population) to match the data presented by Ozoh et al.<sup>15</sup> in the seven study sites 5 or 6 years into community-directed treatment with ivermectin (CDTI) (see Table 2 of the Main Text). Solid lines are the means of 1,000 model runs; shaded areas are the 95% uncertainty intervals (2.5th to 97.5th quantiles of stochastic model predictions); black circles are estimates with Clopper-Pearson 95% confidence intervals. These results were used to model the impact of CDTI on onchocerciasis skin disease (OSD) presented in Figs. 5-8 of the Main Text. NB: y-axis in different scales.

## Supplementary Text 5. Modelling for policy: PRIME-NTD

We adhered to the Five Principles of the Neglected Tropical Diseases (NTD) Modelling Consortium for good practice in policy-relevant NTD modelling<sup>21</sup> when conducting this research. Table S1 briefly describes the five principles, how they were fulfilled, and where these principles are addressed in the Main Text and/or Supplementary Information.

**Supplementary Table 1.** Policy-Relevant Items for Reporting Models in Epidemiology of Neglected Tropical Diseases (PRIME-NTD) summary table<sup>21</sup>.

| Principle                                | What has been done to satisfy the principle?   | Where in the manuscript is this described?   |
|--|--|--|
| <b>Stakeholder engagement</b>            | Discussions with a range of collaborators, as well as experts in onchocerciasis dermatology and ophthalmology  | Author list, Acknowledgements section  |
| <b>Complete model documentation</b>      | References to the full model description of EPIONCHO-IBM are provided. An Open Access link to the code is provided   | Methods section, Supplementary Information and Code availability section   |
| <b>Complete description of data used</b> | All the data used are published and detailed in the manuscript, with cited references  | Main Text, Supplementary Information, Reference lists of Main Text and Supplementary Information                   |
| <b>Communicating uncertainty</b>         | 95% confidence intervals around prevalence estimates are presented; 95% uncertainty intervals were calculated for 1,000 model repeats for all simulations;<br>To account for uncertainty in transmission settings across study areas, microfilarial and sequela age-prevalence profiles were generated for a range of annual biting rates.<br>For conversion of nodule prevalence into microfilarial prevalence, uncertainty in observed nodule prevalence was incorporated, and 95% credible intervals are presented. | Methods and Results sections, including figures and figure captions in the Main Text and Supplementary Information |
| <b>Testable model outcomes</b>           | Modelled sequela age-prevalence profiles were compared to age-prevalence data. Model outcomes were tested against skin and ocular disease prevalence following annual ivermectin treatment in 9 settings.  | Results and Discussion sections of Main Text. Supplementary Information.   |

## Supplementary References

1. Murdoch, M. E., Murdoch, I. E., Evans, J., Yahaya, H., Njepuome, N., Cousens, S., Jones, B. R. & Abiose, A. Pre-control relationship of onchocercal skin disease with onchocercal infection in Guinea Savanna, Northern Nigeria. *PLoS Negl. Trop. Dis.* **11**, e0005489 (2017).
2. Brown, L. D., Cat, T. T. & DasGupta, A. Interval estimation for a proportion. *Stat. Sci.* **16**, 101–133 (2001).
3. Hamley, J. I. D., Milton, P., Walker, M. & Basáñez, M.-G. Modelling exposure heterogeneity and density dependence in onchocerciasis using a novel individual-based transmission model, EPIONCHO-IBM: implications for elimination and data needs. *PLoS Negl. Trop. Dis.* **13**, e0007557 (2019).
4. Filipe, J. A. N., Boussinesq, M., Renz, A., Collins, R. C., Vivas-Martinez, S., Grillet, M. E., Little, M. P. & Basáñez, M.-G. Human infection patterns and heterogeneous exposure in river blindness. *Proc. Natl. Acad. Sci. U. S. A.* **2005**; **102**, 15265–15270 (2005).
5. Basáñez, M.-G., Walker, M., Turner, H. C., Coffeng, L. E., de Vlas, S. J. & Stolk, W. A. River blindness: mathematical models for control and elimination. *Adv. Parasitol.* **94**, 247–341 (2016).
6. Walker, M., Stolk, W. A., Dixon, M. A., Bottomley, C., Diawara, L., Traoré, M. O., de Vlas, S. J. & Basáñez, M.-G. Modelling the elimination of river blindness using long-term epidemiological and programmatic data from Mali and Senegal. *Epidemics* **18**, 4–15 (2017).
7. Turner, H. C., Walker, M., Churcher, T. S. & Basáñez, M.-G. Modelling the impact of ivermectin on River Blindness and its burden of morbidity and mortality in African Savannah: EpiOncho projections. *Parasit. Vectors* **7**, 241 (2014).
8. Little, M. P., Breitling, L. P., Basáñez, M.-G., Alley, E. S. & Boatin, B. A. Association between microfilarial load and excess mortality in onchocerciasis: an epidemiological study. *Lancet* **363**, 1514–1521 (2004).
9. Walker, M., Little, M. P., Wagner, K. S., Soumbey-Alley, E. W., Boatin, B. A. & Basáñez, M.-G. Density-dependent mortality of the human host in onchocerciasis: relationships between microfilarial load and excess mortality. *PLoS Negl. Trop. Dis.* **6**, e1578 (2012).
10. Hamley, J. I. D., Walker, M., Coffeng, L. E., Milton, P., de Vlas, S. J., Stolk, W. A. & Basáñez, M.-G. Structural uncertainty in onchocerciasis transmission models influences the estimation of elimination thresholds and selection of age groups for seromonitoring. *J. Infect. Dis.* **221**(Suppl 5), S510–S518 (2020).
11. Dietz, K. Density-dependence in parasite transmission dynamics. *Parasitol. Today* **4**, 91–97 (1988).
12. Churcher, T. S., Filipe, J. A. N. & Basáñez, M.-G. Density dependence and the control of helminth parasites. *J. Anim. Ecol.* **75**, 1313–1320 (2006).
13. Dietz, K. The population dynamics of onchocerciasis. In Population dynamics of infectious diseases (ed. R. M. Anderson), pp. 209–241. London: Chapman & Hall (1982).

14. Dyson, L., Stolk, W. A., Farrell, S. H. & Hollingsworth, T. D. Measuring and modelling the effects of systematic non-adherence to mass drug administration. *Epidemics* **8**, 56–66 (2017).
15. Ozoh, G. A., Murdoch, M. E., Bissek, A. C., Hagan, M., Ogbuagu, K., Shamad, M., Braide, E. I., Boussinesq, M., Noma, M. M., Murdoch, I. E., Sékétéli, A. & Amazigo, U. V. The African Programme for Onchocerciasis Control: impact on onchocercal skin disease. *Trop. Med. Int. Health* **16**, 875–883 (2011).
16. Prost A. Latence parasitaire dans l'onchocercose. *Bull. World Health Organ.* **58**, 923–925 (1980).
17. Little, M. P., Basáñez, M.-G., Breitling, L. P., Boatin, B. A. & Alley, E. S. Incidence of blindness during the Onchocerciasis control programme in western Africa, 1971-2002. *J. Infect. Dis.* **189**, 1932–1941 (2004).
18. Coffeng, L. E. Onchocerciasis: the pre-control association between prevalence of palpable nodules and skin microfilariae - technical note and posterior draws for conversion equation. <https://zenodo.org/records/13969100>; <https://doi.org/10.5281/zenodo.13969100> (2024).
19. Coffeng, L. E., Pion, S. D. S., O'Hanlon, S., Cousens, S., Abiose, A. O., Fischer, P. U., Remme, J. H. F., Dadzie, K. Y., Murdoch, M. E., de Vlas, S. J., Basáñez, M.-G., Stolk, W. A. & Boussinesq, M. Onchocerciasis: the pre-control association between prevalence of palpable nodules and skin microfilariae. *PLoS Negl. Trop. Dis.* **7**, e2168 (2013).
20. Kirkwood, B., Smith, P., Marshall, T. & Prost, A. Variations in the prevalence and intensity of microfilarial infections by age, sex, place and time in the area of the Onchocerciasis Control Programme. *Trans. R. Soc. Trop. Med. Hyg.* **77**, 857–861 (1983).
21. Behrend, M. R., Basáñez, M.-G., Hamley, J. I. D., Porco, T. C., Stolk, W. A., Walker, M., de Vlas, S. J. & NTD Modelling Consortium. Modelling for policy: the five principles of the Neglected Tropical Diseases Modelling Consortium. *PLoS Negl. Trop. Dis.* **14**, e0008033 (2020).